

INFLUENCE OF HEATING MODE ON THE NANOPARTICLE DEPOSITION AND ON THE BOILING HEAT TRANSFER USING NANOCOATED SURFACES

Mogaji Taye Stephen

UNESP – São Paulo State University, Department of Mechanical Engineering, Av. Brasil, 56, 15385-000, Ilha Solteira, SP, Brazil
 mogajits@gmail.com

Leonardo Lachi Manetti

UNESP – São Paulo State University, Department of Mechanical Engineering, Av. Brasil, 56, 15385-000, Ilha Solteira, SP, Brazil
 leomanetti@hotmail.com

Igor Seicho Kiyomura

UNESP – São Paulo State University, Department of Mechanical Engineering, Av. Brasil, 56, 15385-000, Ilha Solteira, SP, Brazil
 igorseicho@gmail.com

***Elaine Maria Cardoso** (*Corresponding author)

UNESP – São Paulo State University, Department of Mechanical Engineering, Av. Brasil, 56, 15385-000, Ilha Solteira, SP, Brazil
 elainemaria@dem.feis.unesp.br

Abstract. *This work aims to analyze the heat transfer performance during pool boiling of DI water on copper surfaces coated with maghemite nanoparticles. The nanocoated surfaces were produced by maghemite nanoparticle deposition, for different mass concentrations (0.029 and 0.29 g/l, corresponding to low and high nanofluid concentration, respectively), via boiling process of Fe₂O₃-deionized water nanofluid. Two sets of experiments were performed in this study to reveal the potential effect of nanoparticles deposition on the heat transfer. (i) Firstly, pool boiling of Fe₂O₃-DI water nanofluid were carried out on copper surface by applying heat flux in steps ranged from 100 to 800 kW/m²; and secondly, by applying a fixed heat flux of 500 kW/m². (ii) After the deposition process, pool boiling experiments were carried out on each of the copper surfaces coated with maghemite nanoparticles using deionized water as working fluid at atmospheric pressure and under saturated conditions. All samples were submitted to metallographic, roughness and wettability analysis. Changes in the boiling surface morphology, wettability and thermal resistance of the heating surface owing to nanoparticles deposition are dependent on the heating mode. Besides, as the nanofluid concentration increases the surface roughness also increases, and the higher the nanofluid concentration, the lower the contact angle of water on the coated surface. The heat transfer performance depends on the nanofluid concentration, the original surface roughness and the heating mode.*

Keywords: *pool boiling, heat transfer coefficient, Fe₂O₃-deionized water nanofluid.*

1. INTRODUCTION

The enhancement of nucleate boiling using different treated surfaces has been an interesting challenge for researchers looking for industrial applications, particularly in microelectronics, which combines miniaturization with a volume restriction for the cooling liquid.

Several researchers have been conducting tests on nucleate pool boiling using nanostructured surfaces. Those researchers generally accept the idea of an enhancement in the CHF (Dinh *et al.*, 2004; Wen and Ding, 2005; Heitich *et al.*, 2014; Souza *et al.*, 2014). However, the same cannot be said for the HTC, because different results have been observed during pool boiling on nanostructured surfaces (Heitich *et al.*, 2014; Souza *et al.*, 2014; Bang and Chang, 2005; Kim *et al.*, 2007; Ahmed and Hamed, 2012). Heitich *et al.* (2014) analyzed the effect of nanostructured surfaces on the nucleate boiling of water, at saturation temperature and atmospheric pressure. In the experiment, the nanostructured surface consisted of a Constantan tape nanocoated with molybdenum (achieved by sputtering process) and maghemite (obtained by nanofluid evaporation technique). Intensification in the surface wettability of the nanocoated surfaces was observed, thus causing the CHF to increase. Also, an enhancement in the HTC of the rough surface was detected, whilst for the other surfaces an increase in the HTC was achieved only for high heat fluxes.

Souza *et al.* (2014) studied the effect of the deposition of γ -Fe₂O₃ nanoparticles (10 and 80 nm diameter) on a horizontal surface ($R_a = 0.16 \mu\text{m}$), using HFE7100 as working fluid. In this experiment, two main conditions were considered - unconfined and confined boiling. A HTC increment was found for the nanostructured surface with smaller nanoparticles as compared to the surface without deposition. The results for the larger nanoparticles showed a decrease in the HTC as compared to the case without deposition. The authors then concluded that the microstructure of the heating surface, corresponding to quantity and size of surface defects, influences the heat transfer process.

Others authors (Bang and Chang, 2005; Kim *et al.*, 2007; Ahmed and Hamed, 2012) varied the concentration of the nanofluids for a fixed value of nanoparticle diameter and surface roughness, and they reported a deterioration in the

HTC. Ahmed and Hamed (2012) pointed out that the nanofluid concentration is also an important parameter to be considered in nanofluid pool boiling studies, since the deposition of nanoparticles occurs at a slower rate for low concentration of nanofluids (0.01 vol.%), then resulting in a HTC enhancement. This behavior is due to the thermal conductivity of nanofluids being more dominant than the nanoparticle deposition on the surface.

The modification in the behavior of both the CHF and HTC can be explained by the changes in the surface wettability and the number of microcavities caused by the nanostructured surface. In the case of the CHF enhancement, the nanoparticles deposition improved the wettability of the heating surface (Kim and Kim, 2007, Golubovic *et al.*, 2009, Kiyomura *et al.*, 2015, Park *et al.*, 2014), thus allowing the fluid located near the surface to rewet the hot spots and to cool down the heating surface. Regarding the modifications in the HTC, the nanoparticles deposition generated a porous layer on the heating surface that led to a change in the surface roughness and in the number of microcavities. Some recent works have shown that the HTC behavior also depends on the contact angle, since the bubble frequency and its departure diameter decreases with the nanostructure layer, as summarized by Ignácio *et al.* (2015).

Kiyomura *et al.* (2016) carried out pool boiling experiments using copper surfaces with different roughnesses and deionized water as the working fluid under saturated conditions. The nanostructured surfaces were produced by boiling process of Fe₂O₃-water based nanofluid, with different nanofluid concentrations. According to the authors, the highest HTC were obtained for the nanocoated smooth surface (at low nanofluid concentrations).

The aim of this work is to analyze the effect of the heating mode on the nanocoating process by using the nanofluid pool boiling technique, as well as the effects on the HTC behavior for the nucleate boiling regime of water.

2. MATERIALS AND METHODS

2.1 Pool boiling apparatus

In the present study, the boiling chamber (Fig.1) consists of a glass cube involving a hollow borosilicate glass tube with an internal diameter of 90 mm, 180 mm in height, and wall thickness of 10 mm.

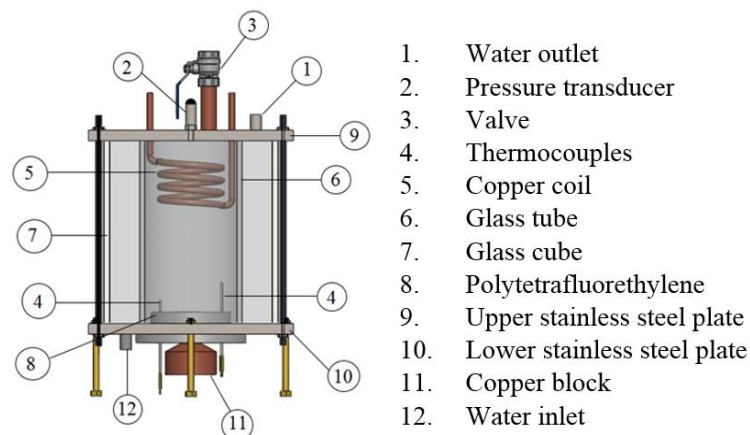


Figure 1. Pool boiling apparatus.

In the gap between the glass cube and the glass tube there is a forced flow of water whose temperature is controlled by a thermostatic bath, in order to maintain the temperature of the working fluid close to the saturation temperature. A second thermostatic bath is used to control the temperature of the condenser located at the top of the boiling chamber. A pressure transducer measures the pressure inside the boiling chamber, which must be maintained at local atmospheric pressure during the boiling tests.

The test section consists of a copper block (20 mm diameter and 60 mm height) containing three thermocouples type K fixed inside holes at the radial center of the copper cylinder, to determine the wall temperatures and the heat flux. The copper block is heated by a cartridge resistance (with a maximum power of 300 W at 220 V applied). The thermal insulation of the test section consists of polytetrafluorethylene and vermiculite. Figure 2 shows the test section assembly.

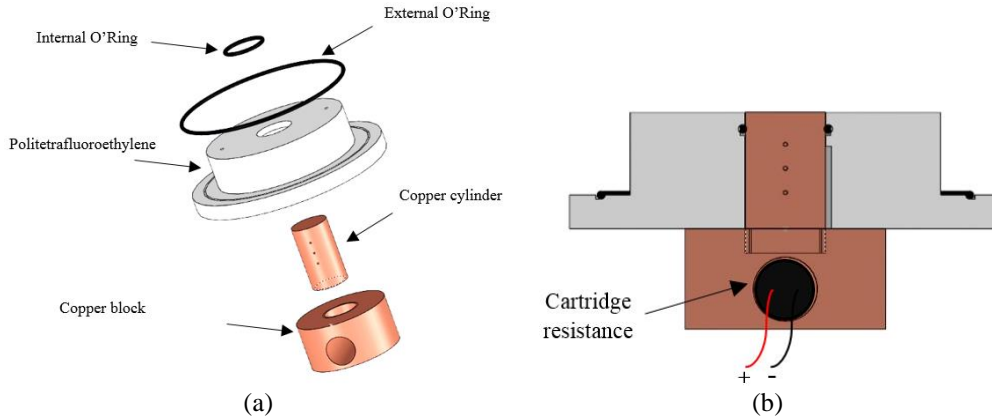


Figure 2. Test section assembly (a) exploded view. (b) cut view.

The temperature readings were acquired from the thermocouples by the data acquisition system Agilent 34970A. Each test had duration of 1500 s for each heat flux applied, but only the temperature data for the last 500 s (corresponding to 100 experimental data points) of the test interval were acquired, in order to ensure the steady state regime was achieved.

The heat transfer coefficient was calculated using the Newton's law of cooling given by:

$$h = \frac{q''}{T_w - T_{sat}(p_{atm})} \quad (1)$$

where T_w is the measured temperature, and $T_{sat}(p_{atm})$ corresponds to the saturation temperature of the water at atmospheric pressure.

2.2 Test surface preparation

The copper surfaces were polished using two different methods, one corresponding to a smooth surface ($R_a = 0.05 \mu\text{m}$, namely SS), which was mechanically polished, and a rough surface ($R_a = 0.23 \mu\text{m}$, namely RS), which was manually polished.

The polished copper heater surfaces namely SS and RS were coated with maghemite nanoparticle during pool boiling of Fe_2O_3 -water nanofluid using different heating modes: by applying a varying heat flux (VHF) ranged from 100 to 800 kW/m^2 and, by applying a fixed heat flux (FHF) at 500 kW/m^2 . In order to verify the influence of nanoparticles layer thickness on the surface roughness and wettability, two different nanofluids concentrations were used: 0.029 g/l (corresponding to low nanofluid concentration, LC) and 0.29 g/l (corresponding to high nanofluid concentration, HC). The Fe_2O_3 -water based nanofluid, with an average particle size of 10 nm, was supplied by the NFA/Instituto de Física - Universidade de Brasília.

Ten different copper surfaces, eight of them being nanostructured, were analyzed. These surfaces consisted of one smooth surface (SS), one rough surface (RS), two smooth surfaces with nanoparticle deposition by varying heat flux (at low and high nanofluid concentrations, VHF-SS-LC and VHF-SS-HC, respectively), two smooth surfaces with nanoparticle deposition by fixed heat flux (at low and high nanofluid concentrations, FHF-SS-LC and FHF-SS-HC, respectively), two rough surfaces with nanoparticle deposition by varying heat flux (at low and high nanofluid concentrations, VHF-RS-LC and VHF-RS-HC, respectively) and two rough surfaces with nanoparticle deposition by fixed heat flux (at low and high nanofluid concentrations, FHF-RS-LC and FHF-RS-HC, respectively).

In the present study the nanostructured surface was obtained through a process of vigorous boiling of nanofluid for two different mass concentrations and for two different heating modes. After that, the nanofluid was removed from the boiling chamber and the modified heating surface was used in the boiling tests without removing the layer of deposited nanoparticles. Thus, experimental tests were performed to investigate the potential effect of nanoparticles deposition on the pool boiling heat transfer. The experiments were conducted using deionized water as the working fluid under saturated conditions at atmospheric pressure.

The same procedure was applied to all samples in order to ensure repeatability. The temperature uncertainty was $\pm 0.4 \text{ }^\circ\text{C}$. For all surfaces tested, the experimental uncertainty for the heat flux and for the heat transfer coefficient varied from 15.3 % to 1.6 %, and from 15.9 % to 2.6 % respectively.

2.3 Surface characterization technique

Prior and after each test, different techniques were used to obtain the surfaces characteristics such as, scanning electron microscope (SEM), surface roughness (R_a) by a rugosimeter and static contact angles measurements by analysis of pictures of a sessile droplet of water using image post processing software. The scanning electron microscope (SEM) and surface roughness (R_a) characteristics were performed by using EVOLS15 Zeiss® with a magnification of 1000x and rugosimeter (Mitutoyo Surftest SJ 301 model) with measuring range of $-200 \mu\text{m}$ to $+150 \mu\text{m}$ (uncertainty of $\pm 0.005 \mu\text{m}$), respectively.

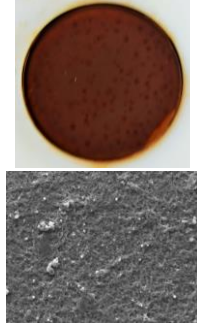
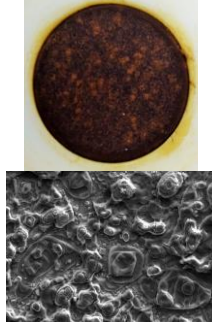
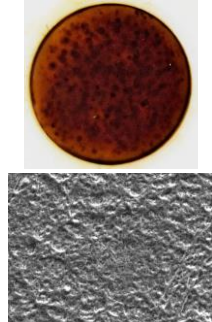
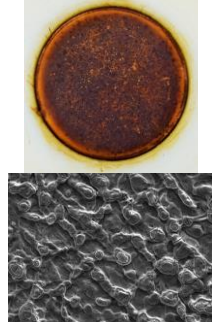
Surfaces	Before nanofluid pool boiling	After nanofluid pool boiling at of 500 kW/m^2 (FHF)	After nanofluid pool boiling ranged from 100 to 800 kW/m^2 (VHF)
Smooth surface (SS-LC)	 $R_a = 0.05 \mu\text{m}$	 $R_a = 0.23 \mu\text{m}$	 $R_a = 0.48 \mu\text{m}$
Smooth surface (SS-HC)	 $R_a = 0.05 \mu\text{m}$	 $R_a = 0.46 \mu\text{m}$	 $R_a = 1.51 \mu\text{m}$
Rough surface (RS-LC)	 $R_a = 0.23 \mu\text{m}$	 $R_a = 0.24 \mu\text{m}$	 $R_a = 0.38 \mu\text{m}$
Rough surface (RS-HC)	 $R_a = 0.23 \mu\text{m}$	 $R_a = 0.43 \mu\text{m}$	 $R_a = 0.80 \mu\text{m}$

Figure 3. SEM images of smooth and rough surfaces, before and after nanofluid pool boiling, with two different mass concentrations and for two different heating modes.

Figure 3 shows the surface condition for smooth and rough copper surface before and after the pool boiling of Fe_2O_3 -water based nanofluid experiments for two different mass concentrations and for two different heating modes.

The apparatus used to measure the static contact angle as shown in Fig. 4 consists of a test surface, a camera, a green LED light source, a light diffuser and an aluminum plate where the test surface is fixed. The measurements were made for two different randomly selected locations on the surfaces. The pictures were analyzed using the same procedure as described by Kiyomura et al. (2016).

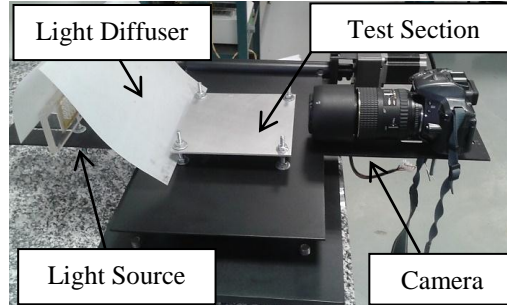


Figure 4. Experimental apparatus to measure the contact angle.

2.4 Boiling apparatus validation

In order to validate the pool boiling apparatus, tests were carried out for DI water on the smooth (SS) and rough (RS) heating surfaces. The experimental values, the curve fitting and the predicted values are plotted in Fig. 5. The curve fitting was based on the relation between the heat transfer coefficient and the heat flux, expressed as follows:

$$h = C q'^n \quad (2)$$

where C is a coefficient dependent on the surface-fluid interaction and n is an exponent of the heat flux. The predicted values of the heat transfer coefficient are given by the Rohsenow's (1952) correlation as follows:

$$h = \frac{1}{C_{sf}} Pr_l^{-s} \frac{q'' c_{pl}}{h_{lv}} \left(\frac{\mu_l h_{lv}}{q''} \right)^r \left[\frac{\sigma}{g(\rho_l - \rho_v)} \right]^{-\frac{1}{2}r} \quad (3)$$

where $s = 1$ and $r = 1/3$ for water and, μ_l , h_{lv} , c_{pl} , and Pr_l represent the viscosity of the liquid (kg/m.s), the latent heat of vaporization (J/kg), the specific heat of the liquid (J/kg.K) and the Prandtl number of the liquid, respectively. The thermophysical properties were obtained at local atmospheric pressure ($p_{sat} = 98$ kPa). C_{sf} is a coefficient that depends on the material of the heating surface, the surface roughness and the working fluid.

As suggested by Vachon *et al.* (1968), the authors assumed C_{sf} values of 0.0147 and 0.0107 for SS and RS, respectively. As shown in Fig. 5, the predicted values agree well with the experimental data with a mean absolute error (MAE) of about 4% for smooth surface and 7% for rough surface. It can be noticed that the values of n obtained using Eq. (2) is about 0.77, agreeing with Stephan (1992) who reported that, in the nucleate boiling regime, the value of n generally lies between 0.6 and 0.8.

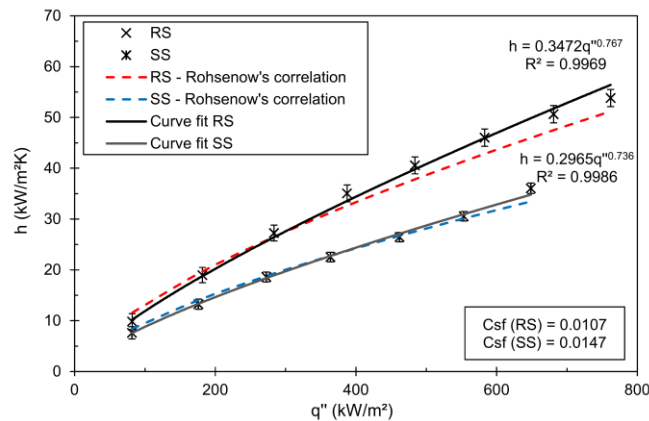


Figure 5. Pool boiling apparatus validation for both smooth and rough surfaces.

3. RESULTS AND DISCUSSION

Figures 6 and 7 show the pool boiling curves obtained for the smooth and rough surfaces (without deposition) and nanocoated surfaces. As can be seen in Fig. 6, the nanocoated surfaces showed a better heat transfer performance than the smooth one; moreover, the deposition process also affected the pool boiling performance results.

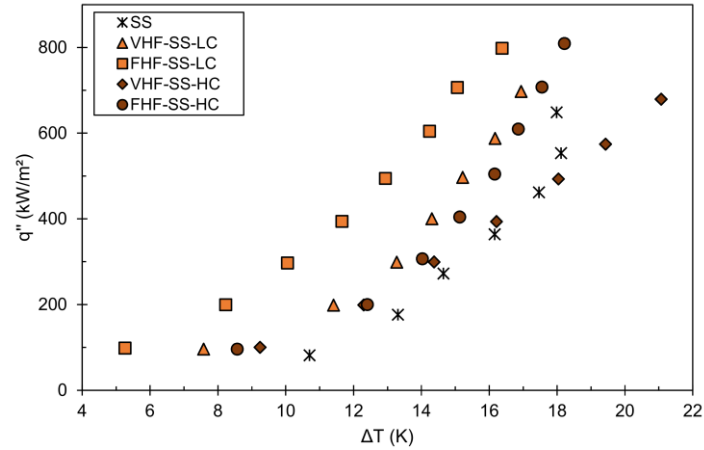


Figure 6. Pool boiling curves for water on smooth surface with different characteristics and for different heating modes.

In Figure 7, the nanocoated rough surfaces showed a worse heat transfer performance than the rough surface (without deposition); however, a lower wall superheating temperature was observed for the FHF nanoparticle deposition method compared with the VHF nanoparticle deposition method.

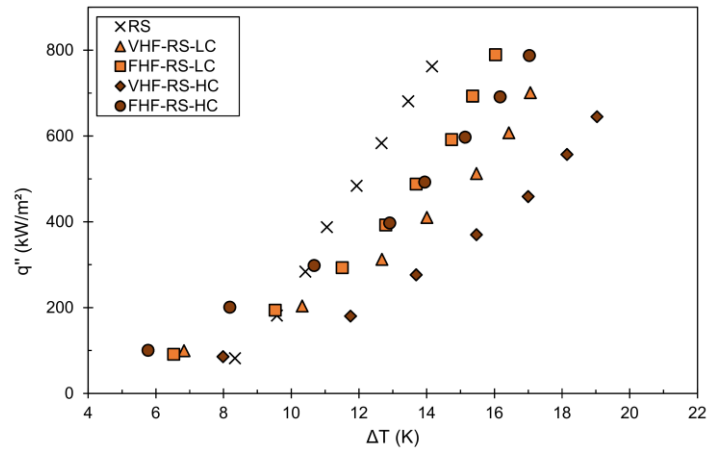


Figure 7. Pool boiling curves for water on rough surface with different characteristics and for different heating modes.

The HTC degradation observed for the nanocoated rough surfaces obtained through VHF nanoparticle deposition method may be due to the thicker nanolayer deposited on the heating surface. The pool boiling of Fe_2O_3 -water nanofluid by applying a varying heat flux (VHF) increases the nanoparticle deposition rate for high heat flux values increasing the nanolayer thickness and, consequently, the thermal resistance of the heating surface. In addition, the nanofluid concentrations used for the coating process also play an important role on the surface changing morphology, since the low concentration nanofluid showed a higher heat transfer coefficient. These behaviors are consistent with those observed in the studies of Ahmed and Hamed (2012) and Vafaei (2015).

Taking into account only the nanostructured surfaces, the decrease in the wall superheat temperature and enhancement in pool boiling performance was observed to be more pronounced with the FHF nanoparticle deposition method independently of the original surface roughness considered in the present study.

The analyzes of the changes in the heating surface morphology considering their roughness and wettability before and after the coating process are presented in Fig. 8 and Fig. 9.

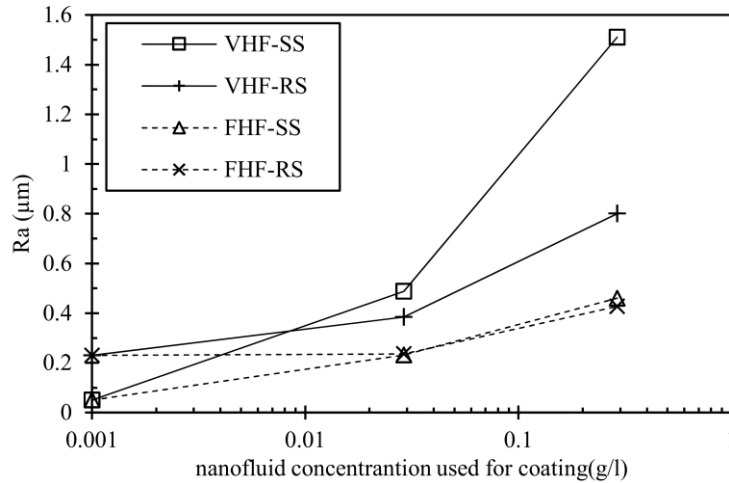


Figure 8. Heating surface roughness (R_a) before and after coating process for different nanofluid concentrations.

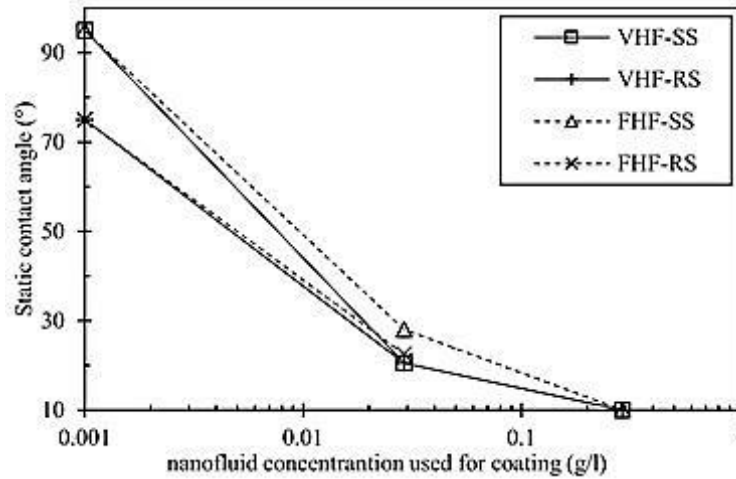


Figure 9. Static contact angle for smooth, rough and nanocoated surfaces using water droplet.

According to the results displayed in Figs. 8 and 9, the roughness of the nanocoated surface and the static contact angle are function of the nanofluid concentration and the original surface condition. As the nanofluid concentration increases the surface roughness (R_a) also increases, independently of the heating mode. This increase is more pronounced for the VHF nanoparticle deposition method and smooth surface. This behavior is mainly related to the increase in the nucleation site density, due to changes in the surface morphology during nanofluid pool boiling, leading to a better heat transfer performance compared to the smooth surface (without deposition), as shown in Fig. 6.

Moreover, according to the static contact angle measurements, the contact angle decreases with increasing nanofluid volumetric concentration, for both smooth and rough surfaces and independently of the heating mode, such finding indicates an increase in the wettability.

4. CONCLUSION

In order to evaluate the effects of heating mode on nanoparticles deposition and on the HTC behavior, two methods were used to produce the nanostructured surfaces by nanofluid boiling process: one by varying the heat flux (VHF) and another by fixing the heat flux (FHF) applied. The pool boiling curves, using water as the working fluid, showed that the FHF method is able to deposit nanoparticles in such a way that the wall superheat is lower than the nanostructured surfaces produced by the VHF method. This implies that, compared with the nanocoated surfaces produced by the VHF method, higher heat flux can be achieved by using the nanocoated surfaces produced by the FHF method with relatively low surface superheating which could improve the efficiency and the safety margin of the thermal systems.

The smooth nanocoated surfaces showed a better heat transfer performance than the smooth surface without deposition, independently of the heating mode. For the rough surfaces, all the nanostructured samples showed a decrease in the HTC compared to the rough surface without deposition, indicating that the thickness of the covering

layer deposited on the surface increases, leading to an enhancement of the thermal resistance with consequent degradation of the HTC.

5. ACKNOWLEDGEMENTS

The authors are grateful for the financial support from the PPGEM – UNESP/FEIS, from the National Council of Technological and Scientific Development of Brazil (CNPq grant number 458702/2014-5), from FAPESP (grant numbers 2013/15431-7 and 2014/19497-5) and from a CAPES sponsored post-doctoral fellowship for Mogaji T.S.

6. REFERENCES

- Ahmed, O. and Hamed, M. S., 2012. Experimental investigation of the effect of particle deposition on pool boiling of nanofluids, *International Journal of Heat Mass Transfer*, Vol. 55, p. 3423-3436.
- Bang, I. C. and Chang, S. H., 2005. Boiling heat transfer performance and phenomena of Al₂O₃ – water nanofluids from a plain surface in a pool, *International Journal of Heat Mass Transfer*, Vol. 48, p. 2407-2419.
- Barber, J., Brutin, D. and Tadrist, 2011. A review on boiling heat transfer enhancement with nanofluids. *Nanoscale Research Letters*, Vol. 6, p. 280.
- Dinh, N., Tu, J. and Theofanous T., 2004. "Hydrodynamic and physicochemical nature of burnout in pool boiling". In *Proceedings of the 5th International Conference on Multiphase Flow, Yokohama, Japan, 2004*. Counsel of Technological and Scientific
- Golubovic, M. N., Hettiarachchi, H. M., Worek, W. M., Minkowycz, W. J., 2009. Nanofluids and critical heat flux, experimental and analytical study, *Applied Thermal Engineering*, Vol.29, p. 1281-1288.
- Heitich, L.V., Passos, J.C., Cardoso, E.M., Silva, M.F., Klein, A.N., 2014. Nucleate boiling of water using nanostructured surfaces, *Journal of the Brazilian Society of Mechanical Sciences and Engineering*, Vol 36, p. 181-192
- Ignácio, I., Cardoso, E. M., Gasche, J.L., Ribatski, G., 2015. "A state-of-art review on pool boiling on nanostructured surfaces". In *Proceedings of the 12th International Conference on Nanochannels, Microchannels, and Minichannels, ASME 2015*. San Francisco, California, USA, InterPACKICNMM2015 – 48120.
- Kim, H. D. and Kim, M. H., 2007. Effect of nanoparticle deposition on capillary wicking that influences the critical heat flux in nanofluids, *Applied Physics Letters*, Vol. 91, p. 014104.
- Kim, S. J., Bang, I. C., Buongiorno, J., Hu, L.W., 2007. Surface wettability change during pool boiling of nanofluids and its effect on critical heat flux, *International Journal of Heat Mass Transfer*, Vol. 50, p. 4105 – 4116.
- Kiyomura, I. S., Nascimento, F. J., Cunha, A. P., Cardoso, E. M., 2015. "Analysis of the influence of surface roughness and nanoparticle concentration on the contact angle" In *Proceedings of 23rd ABCM International Congress of Mechanical Engineering*, Rio de Janeiro, Brazil, 2015.
- Kiyomura, I.S., Manetti, L.L., da Cunha, A.P., Ribatski, G., Cardoso, E.M., 2016. An analysis of the effects of nanoparticles deposition on characteristics of the heating surface and on pool boiling of water, *International Journal of Heat Mass Transfer*, <http://dx.doi.org/10.1016/j.ijheatmasstransfer.2016>.
- Park, S. D., Moon, S. B., Bang, I. C., 2014. Effects of thickness of boiling-induced nanoparticle deposition on the saturation of critical heat flux enhancement, *International Journal of Heat and Mass Transfer*, 78, p. 506-514.
- Rohsenow, W. M., 1952 A Method of Correlating Heat Transfer Data for Surface Boiling Liquids, *Trans. ASME*. Vol. 74, p. 969–976
- Souza, R. R., Passos, J.C., Cardoso, E.M., 2014. Influence of nanoparticle size and gap size on nucleate boiling using HFE7100, *Experimental Thermal and Fluid Science*, Vol. 59, p. 195-201
- Stephan, K., 1992 *Heat transfer in condensation and boiling*, Springer-Verlag, Berlin.
- Vafaei, S., 2015. Nanofluid Pool Boiling Heat Transfer Phenomenon, *Powder Technology*, Vol. 277, p. 181-192.
- Vachon, R.I., Nix, G.H., and Tanger, G.E., 1968 Evaluation of Constants for the Rohsenow Pool-Boiling Correlation, *Journal of Heat Transfer*, 90 p 239.
- Wen, D. and Ding, Y., 2005. Experimental investigation into the pool boiling heat transfer of aqueous based γ -alumina nanofluids, *Journal of Nanoparticle Research*, Vol. 7, p. 265–274.

7. RESPONSIBILITY NOTICE

The authors are the only one responsible for the printed material included in this paper.